

A Missing Value Filling Model Based on Feature Fusion Enhanced Autoencoder

Xinyao LIU, *Shengdong DU, Tianrui LI, Fei TENG
and Yan YANG

School of Computing and Artificial Intelligence, Southwest
Jiaotong University, Chengdu, 611756, P.R.China.

*Corresponding author(s). E-mail(s): sddu@swjtu.edu.cn;

Contributing authors: liuxinyao@my.swjtu.edu.cn;
trli@swjtu.edu.cn; fteng@swjtu.edu.cn; yyang@swjtu.edu.cn;

Abstract

With the advent of the big data era, the data quality problem is becoming more and more crucial. Among many factors, data with missing values is one primary issue, and thus developing effective imputation models is a key topic in the research community. Recently, a major research direction is to employ neural network models such as self-organizing mappings or automatic encoders for filling missing values. However, these classical methods can hardly discover correlation features and common features simultaneously among data attributes. Especially, it is a very typical problem for classical autoencoders that they often learn invalid constant mappings, thus dramatically hurting the filling performance. To solve the above problems, we propose and develop a missing-value-filling model based on a feature-fusion-enhanced autoencoder. We first design and incorporate into an autoencoder a hidden layer that consists of de-tracking neurons and radial basis function neurons, which can enhance the ability to learn correlated features and common features. Besides, we develop a missing value filling strategy based on dynamic clustering (MVDC) that is incorporated into an iterative optimization process. This design can enhance the multi-dimensional feature fusion ability and thus improves the dynamic collaborative missing-value-filling performance. The effectiveness of our model is validated by experimental comparisons to many missing-value-filling methods that are tested on seven datasets with different missing rates.

Keywords: Missing value filling, feature fusion, autoencoder, Radial basis function, Deep neural network.

1 Introduction

Data quality issue is one of the key challenges in many research fields such as data science, data mining, and machine learning. Good-enough data quality is often a prerequisite to many downstream tasks. If this issue is not handled properly, it will lead to unexpected outcomes generated or even wrong conclusions drawn, known as the “Garbage In Garbage Out” problem [1]. Among many factors, data containing missing values is one primary reason that affects data quality and has received enormous attention from the research community. Many real-world applications do generate incomplete or fragmented data pieces [2] but most learning models do not readily work with missing values. Therefore, many researchers have proposed and developed various missing-value-filling methods from different perspectives [3][4][5]. The principle is to properly estimate the distribution of missing values and then induce deterministic numbers from the uncertainty.

While many missing value estimations are based on conventional statistical models, the recent advances of deep learning models have provided a new perspective [6]. Deep neural nets are very strong in non-linearity approximation, and even simple models can achieve reasonable performance. To name some early works: Self-Organizing Map (SOM) [3], Multi-Layer Perceptron (MLP) [4], and AutoEncoder (AE) [5]. On the other hand, simple models are also limited. For example, the SOM model ignores the correlation among data attributes, thus resulting in low model accuracy [7]; the MLP-based model although has considered data attribute correlation, its training process is overly time-consuming because of its high computational complexity; lastly, of the most relevance to our work, the AE-based model above has effectively reduced the model complexity by implementing only one network structure, but the model outputs are likely to track the corresponding inputs, thus leading to an invalid identity mapping learned and showing the self-tracking problem [8]. Hence, many improvements have been made upon the basic autoencoder-based model. For instance, Radial Basis Function Neural Network (RBFNN) [9], Generalized Regression Neural Network (GRNN) [9], Counterpropagation Network (CPN) [10], Tracking-removed Autoencoder (TRAЕ)[8], and Correlation-enhanced Auto-associative Neural Network (CE-AANN)[11]. However, the above methods could hardly learn the common features and the interrelated features simultaneously. Especially when using a only basic autoencoder to fill missing values, it often learns invalid constant mappings.¹

¹This paper is an extended version of [12], which has been accepted for presentation at the 15th International FLINS Conferences on Machine learning, Multi agent and Cyber physical systems (FLINS2022).

To address the aforementioned problems, this paper proposes a feature-fusion-enhanced and autoencoder-based missing-value-imputation model (FFEAM). The first novelty is that we incorporate a hidden layer comprised of de-tracking neurons and radial basis function neurons, which can enhance the multi-dimensional feature fusion ability. De-tracking neurons can avoid learning invalid constant mappings that often occur in classical autoencoders; besides, the neurons can also explore the interrelated features among data attributes effectively. Radial basis function neurons are designed to have an automatic clustering ability, which can better learn the common features among data missing samples. The outputs of these two types of neurons are further constrained by each other, and thus the model can simultaneously discover common features and interrelated features among data attributes. The second novelty is that we develop a missing value filling strategy based on dynamic clustering (MVDC) that is incorporated into an iterative optimization process. Specifically, during each iteration, clustering is performed on the current training data, and the selected centroids and widths are fed to the radial basis function neurons; meanwhile, missing values are treated as variables along with the model parameters that are together optimized. As the optimization proceeds, the estimation of the missing values will be more accurate, and thus the filling precision will gradually improve.

The main contributions of this paper can be summarized as follows:

- We propose a missing value filling model based on a feature-fusion-enhanced autoencoder. We address the typical problem occurring in classical autoencoders by adding a hidden layer that consists of de-tracking neurons and radial basis function neurons. These two types of neurons can jointly enhance the abilities of learning correlated features and common features among data.
- We develop a missing value filling strategy based on dynamic clustering (MVDC) that is incorporated into an iterative optimization process. This design can enhance the multi-dimensional feature fusion ability and thus improves the dynamic collaborative missing-value-filling performance.
- We conduct extensive experiments with seven datasets, of which the results demonstrate that the proposed model achieves a better performance compared to many benchmark models under different missing value conditions.

The rest of this paper is organized as follows. Section 2 introduces the related work. Section 3 first presents the preliminaries and then details the model implementation. Section 4 introduces the architecture of FFEAM. Section 5 validates the effectiveness of the proposed model through comparative experiments, and finally, Section 6 concludes this paper.

2 Related Work

The current popular missing value filling methods can be divided into two categories: statistical models and machine learning models [13]. In the first category, the classical method is the mean filling method, which mostly uses the average value of data attribute column to fill in the missing values, and the average value of all existing values in the incomplete attribute column will be used as the filling value for numerical data, and the mode filling value will be used for non-numerical missing data [14]. Regression imputation model is another common statistical method, which uses attributes with missing values as dependent variables and other attributes as independent variables, and uses the correlation between them to model and solve parameters to fill in missing values [15]. The Expectation-Maximization (EM) filling method uses the marginal distribution of the available data to perform the Maximum Likelihood Estimate (MLE) on the missing data to analyze the most likely value to be obtained for the missing value filling [15]. In the research of missing value filling models based on machine learning, K-Nearest Neighbors (KNN) is one of the classical methods, and its main idea is to select the top K categories with the least variance by sorting the variance between the categorical samples and the training samples from smallest to largest [16]. Tutz et al. proposed a weight parameter adjustment method to optimize the weight between samples under different K values to improve the effect of missing value filling [17]. The ordered nearest neighbor filling method is an improvement to the KNN filling method, which adopts the strategy of filling and expanding, and can use the complete data samples obtained by filling the previous missing data, also improves the data utilization rate [18]. Gajawada et al. proposed a cluster filling method that uses a K-Means clustering model to divide the input dataset into K clusters, and for each missing data, a set of nearest neighbors of that data is found in the cluster to which it belongs, and the average of the nearest neighbors is used for missing value filling [19]. Yi et al. proposed a missing value filling method based on spatio-temporal multi-view learning, which automatically fill missing records of geosensing data by learning from multiple views from both local and global perspectives [20].

Since the deep learning method was proposed in 2006, it has attracted the attention of researchers [21]. The deep learning model can automatically extract and learn the deep features in the data through the multi-layer neural network [22]. Currently, deep learning-based missing value filling methods are becoming a hot research topic [23]. For instance, Ravi et al proposed more variants of classical autoencoder models for missing value filling, and the experiments demonstrated that the generalized regression autoencoder has better filling performance in the family of autoencoder-based architectures [14]. However, the generalized regression autoencoder has high computational complexity due to the need to repeatedly calculate the distance between incomplete data and all complete data during filling. Considering that the classical autoencoder has a certain dependence on the model input and may learn invalid constant mappings. In order to reasonably weaken the tracking of the

input by the autoencoder, Lai et al. developed a dynamic filling method for the de-tracking autoencoder, whose hidden layer neurons can avoid the self-tracking of the network output to the corresponding input by dynamically organizing the input structure [8]. Lai et al. also continued their improvement to propose the association enhanced autoassociative neural network model for missing value filling, which can well explore the association features among data attributes [11].

The above methods such as mean filling [14], K-nearest neighbor filling [16], and clustering-based filling [19] mostly analyze and process the missing data from the data common feature perspective, i.e., fill the data by learning the similarity features between data. Due to its nonlinear feature learning ability, deep neural network can automatically mine complex nonlinear relationships between data attributes, and can learn the correlation features between data attributes to fill in missing values. However, it is difficult for the proposed missing value filling models to perform feature fusion learning from the above two dimensions (common features and correlation features) at the same time.

3 Preliminaries

3.1 Classical autoencoder

Autoencoder(AE) is a classical deep learning model consisting of an encoder and decoder whose output attempts to reconstruct its corresponding input[24]. Since the autoencoder can reproduce the value of the input, if there are missing values in the sample, it can be filled by the value reproduced at the output. The model achieves input reconstruction and missing value filling by minimizing the cost function shown in Equation (1).

$$L = \frac{1}{2n} \sum_{i=1}^n \sum_{j=1}^s (y_{ij} - x_{ij})^2, \quad (1)$$

Where n represents the number of training samples; s represents the number of attributes of the samples; x_{ij} represents the input values, i.e., the data containing pre-filled missing values; and y_{ij} represents the filled values of the model. The model is continuously reduced by training errors, but the reconstructed outputs may learn invalid constant mappings (model outputs and inputs are highly similar or equal), i.e., they may highly track the inputs corresponding to them, presenting self-tracking problem.

3.2 Radial basis function autoencoder

The radial basis function autoencoder consists of an input layer, a single hidden layer, and an output layer [9]. In this model, the connection weight between the input layer and the hidden layer is fixed to 1, while the connection weight between the hidden layer and the output layer is used as a parameter for the training of the model, and the computation process of the radial basis function hidden layer neurons is shown in Equation (2).

$$net_{ik}^{(1)} = \exp \left[-\frac{\|x_i - \mu_k\|}{2\sigma_k^2} \right], k = 1, 2, \dots, n^{(1)}, \quad (2)$$

Where μ_k represents the centroid of the k hidden layer neurons; σ_k is the width of the k hidden layer neurons, which determines the magnitude of the decay of the function taking values along the center to the surrounding. According to the properties of radial basis function, when the input sample is far from the centroid, the activation of the neuron is approximately 0, which belongs to the neuron with low activation. And when the input sample is closer to the center, the activation of the neuron is approximately 1, which belongs to the neuron with high activation. The output layer of the model uses a linear activation function, so the output of the model is approximately equal to the weighted sum of neurons with high activation. The radial basis function autoencoder model has a certain clustering ability, which can explore the common features of data and reduce the self-tracking of the classical autoencoder to a certain extent, but the model is weak in learning the correlation features of data.

3.3 Correlation-enhanced autoassociative neural network

The hidden layer of the the correlation-enhanced autoassociative neural network model(CE-AANN) [11] consists of m_1 traditional hidden layer neurons and m_2 improved hidden layer neurons and produces two outputs in the output layer for both types of neurons. Taking the k th hidden layer neuron as an example, the traditionally hidden layer neuron is solved according to Equation (3).

$$net_{ikj}^{(1)} = \phi \left(\sum_{l=1}^s w_{lk}^{(1)} \cdot x_{il} + b_k^{(1)} \right), j = 1, 2, \dots, s, \quad (3)$$

Where $\phi()$ denotes the activation function of the hidden layer neuron; k represents the k th traditional hidden layer neuron; and s represents the number of attributes. The improved hidden layer neuron is solved according to Equation (4).

$$net_{ikj}^{(1)} = \phi \left(\sum_{l=1, l \neq j}^s w_{lk}^{(1)} \cdot x_{il} + b_k^{(1)} \right), j = 1, 2, \dots, s, \quad (4)$$

Where $\phi()$ denotes the activation function of the hidden layer neuron; k represents the k th improved hidden layer neurons, and s represents the number of attributes. From Equation (4), it can be seen that for the j th neuron in the output layer of the network, the hidden layer neuron dynamically rejects the value of x_{ij} , i.e., the corresponding input of y_{ij} is rejected, and the input values other than x_{ij} are used to solve the hidden layer output.

The cost function of the CE-AANN is shown in Equation (5).

$$L = \frac{1}{2} \sum_{i=1}^n \sum_{j=1}^s [(y_{ij} - x_{ij})^2 + (y_{ij} - r_{ij})^2], \quad (5)$$

Where $y_i = [y_{i1}, y_{i2}, \dots, y_{is}]^T$ denotes the network output; $r_i = [r_{i1}, r_{i2}, \dots, r_{is}]^T$ is the reference output; n represents the total number of data; s represents the number of sample attributes. According to Equation (5), it can be seen that the CE-AANN model constantly minimizes the error between the output y_{ij} and input x_{ij} , and also de-tracked the similarity of input and output, through the mutual constraint of the two types of outputs, the model can weaken the dependence of the output on the input while making the network input have a certain borrowing effect on the output, so as to improve the model's learning ability of data correlation features, but the model is weak in learning common features of the data.

4 Method

4.1 Overall framework of the model

To address the main problems in the classical autoencoder model used for missing value filling, a missing value filling model based on feature fusion enhanced autoencoder is developed, and a novel neural network hidden layer based on de-tracking neurons and radial basis function neurons are designed to collaboratively train to fill missing values. Figure 1 shows the overall framework of the model, which first pre-fills the missing data set by the random forest. The missing values are set as variables by the MVDC filling strategy, and then the samples containing dynamic filling values are input to the FFEAM, which performs two dimensions of fusion learning on the correlation features and common features in the data. Meanwhile, the MVDC filling strategy, through K-means clustering self-organized learning, selects the centroids and variances required for the radial basis function neurons, and finally optimizes the missing filling effect iteratively.

4.2 Feature Fusion Enhanced Autoencoder Design

As shown in Figure 1, the FFEAM contains an input layer, a modified novel hidden layer, and an output layer. in which two types of neurons are developed and jointly constructed: include m_1 de-tracking neurons and m_2 radial basis function neurons. According to the mutual design of the two types of hidden layer neurons, two types of outputs will be generated in the output layer: $y_i = [y_{i1}, y_{i2}, \dots, y_{is}]^T$ represents the output of the network based on the solution of the de-tracking hidden layer neurons, $r_i = [r_{i1}, r_{i2}, \dots, r_{is}]^T$ is the reference output based on the radial basis function hidden layer neuron solution. To introduce the design idea of the novel hidden layer in detail, Figure 2 shows the difference between the conventional neuron, the de-tracking neuron, and the radial basis function neuron with the k th hidden layer neuron as an example.

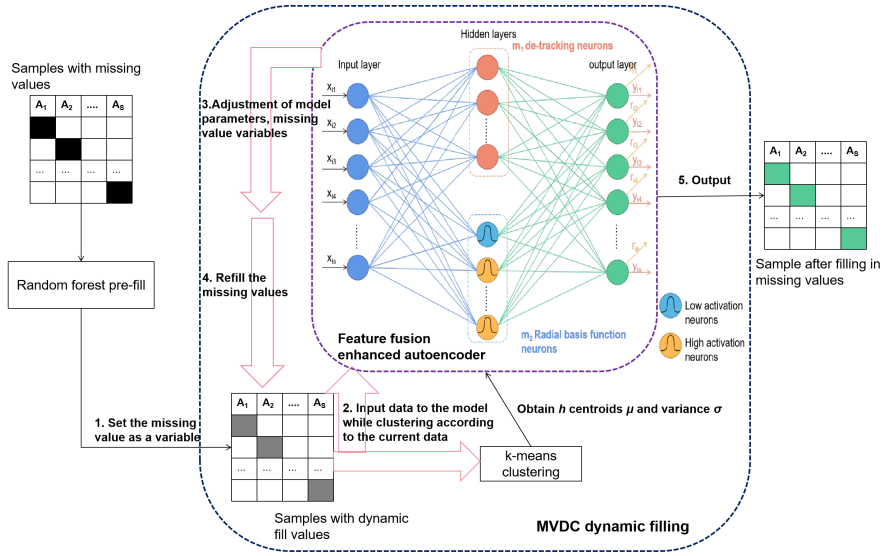


Fig. 1 Design diagram of Feature Fusion Enhanced Autoencoder Model for Missing Value Filling (FFEAM)

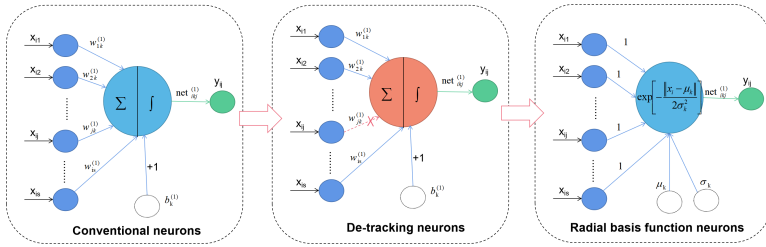


Fig. 2 Three different hidden layer neurons

The FFEAM model comprehensively considers the advantages and disadvantages of various types of neurons and complements the advantages of the two types of neurons through the fusion design of de-tracking neurons and radial basis function neurons. The de-tracking neuron reduces the self-tracking of the classical autoencoder by dynamically eliminating some inputs, and improves the model's learning ability of data correlation features. Moreover, the radial basis function neuron is activated by the radial basis function, and the network reference output can be approximately regarded as the weighted summation of the high activation neurons, which has a certain ability for cluster analysis and exploring the common features of the data. The multi-dimensional feature fusion learning is performed through the complementation

of the above two types of neurons, thereby improving the missing value filling performance.

The whole FFEAM calculation process is described below, the input dataset of the model containing missing values $\{X_{ij} | i=1, 2, \dots, n; j=1, 2, \dots, s\}$, where n is the number of samples and s is the number of attributes, and the missing values X_{ij} are pre-filled using random forest. The method first traverses all the features and starts filling from the column with the least missing. After each regression prediction is completed, the predicted value is put back into the original feature matrix, and then the next feature is filled, and the pre-filling of all missing columns is completed in turn. Then the weights and thresholds of the FFEAM are initialized. Meanwhile, based on the MVDC dynamic filling strategy, the K-means clustering algorithm is used to find h centroids μ_h in the data set after pre-filling, and the width σ_g is calculated by Equation (6).

$$\sigma_g = \frac{c_{max}}{\sqrt{2h}} (g = 1, 2, \dots, h), \quad (6)$$

Where c_{max} denotes the maximum distance between h centers; h represents the number of centers.

Next, the data association features are discovered using the de-tracking neurons in the novel hidden layer, and the data common features are discovered using the radial basis function neurons. The output of the de-tracking neuron is shown in Equation (7).

$$net_{ikj} = \text{relu} \left(\sum_{l=1, l \neq j}^s w_{lk}^{(1)} \cdot x_{il} + b_k^{(1)} \right), j = 1, 2, \dots, s, k = 1, 2, \dots, m_1, \quad (7)$$

Where net_{ikj} represents the output of the k th de-tracking neuron after eliminating the corresponding input x_{ij} , s represents the number of attributes which is the number of columns in the x_{ij} data set, k represents the k th de-tracking neuron, m_1 is the number of de-tracking neurons, $w_{lk}^{(1)}$ represents the connection weight of the l th node in the input layer and the k th de-tracking neuron in the hidden layer, $b_k^{(1)}$ denotes the threshold of the k th de-tracking neuron of the hidden layer; from Equation (7), we can see that for the j th neuron of the output layer, the hidden layer neuron will dynamically reject x_{ij} and use the input values other than x_{ij} to solve the hidden layer output.

The output of the radial basis function hidden layer neuron is shown in Equation (8).

$$net_{igj} = \exp \left[-\frac{\|x_{ij} - \mu_g\|}{2\sigma_g^2} \right], j = 1, 2, \dots, s, g = 1, 2, \dots, m_2, \quad (8)$$

Where net_{igj} represents the output of the g th radial basis function neuron for input x_{ij} , g represents the g th radial basis function neuron, s represents the number of attributes, and m_2 is the number of radial basis function neurons; μ_g is the centroid of the g radial basis function hidden layer neurons, which is

found according to the k-means algorithm. σ_g is the width of the g radial basis function hidden layer neurons, which determine the magnitude of the decay of the function taking values along the center to the surrounding, and is found according to Equation (6).

After the new hidden layer, two types of outputs are obtained in the output layer of the neural network, one is the output y_{ij} of the de-tracking neuron in the corresponding hidden layer, which is calculated according to Equation (9).

$$y_{ij} = \sum_{k=1}^{m_1} w_{kj}^{(2)} net_{ikj} + b_j^{(2)}, j = 1, 2, \dots, s, \quad (9)$$

In the above Equation, net_{ikj} is the output of the k th de-tracking neuron; s is the number of attributes; m_1 is the number of de-tracking neurons, $w_{kj}^{(2)}$ represents the connection weight of the k th de-tracking neuron in the hidden layer and the j th output layer neuron in the output layer, and $b_j^{(2)}$ represents the threshold value between the j th output layer neurons.

Second, the network output r_{ij} corresponding to the radial basis function neuron in the hidden layer is calculated according to Equation (10).

$$r_{ij} = \sum_{g=1}^{m_2} w_{gj}^{(2)} net_{igj} + b_j^{(2)}, j = 1, 2, \dots, s, \quad (10)$$

Where net_{igj} is the output of the g th radial basis function neuron: s is the number of attributes; m_2 is the number of radial basis function neurons; $w_{gj}^{(2)}$ represents the connection weight of the g th radial basis function neuron in the hidden layer and the j th output layer neuron in the output layer, and $b_j^{(2)}$ represents the threshold value between the j th output layer neurons. According to the activation function of Equation (8), when the input sample is far from the centroid, the activation of the neuron is approximately 0, which belongs to the neuron with low activation. And when the input samples are closer to the centroid, the neuron activation is approximately 1, which belongs to the neuron with high activation.

The model loss function is as follows.

$$L = \frac{1}{2} \sum_{i=1}^n \sum_{j=1}^s [(y_{ij} - x_{ij})^2 + (y_{ij} - r_{ij})^2], \quad (11)$$

Through the above computational process, the model minimizes the error between the output y_{ij} and the input x_{ij} while being as close as possible to the reference output of the radial basis function neuron. Through the mutual constraint of the two types of outputs, the model is able to effectively learn the association features and common features in the sample data while weakening the de-tracking of the outputs to the corresponding inputs.

4.3 Description of the algorithm process

FFEAM first fills the missing data set with random forest in advance, sets the missing value as a variable through MVDC filling strategy, and then inputs

the sample containing the dynamic filling value into FFEAM which performs two-dimensional fusion learning on the relevant features and common features in the data. The pseudo code is as follows.

Algorithm 1 FFEAM algorithm

Input: Data sets containing missing values: $\{X_{ij} \mid i=1, 2, \dots, n; j=1, 2, \dots, s\}$.

Output: Filling the complete data set $\{X_{ij} \mid i=1, 2, \dots, n; j=1, 2, \dots, s\}$.

- 1: Pre-filling of missing values X_{ij} using random forest;
 - 2: Initialize the weights w_k and thresholds b_k of FFEAM, set the missing values in X_{ij} as variables;
 - 3: **repeat**()
 - 4: Select the batch sample X_b from the pre-filled sample of missing values;
 - 5: A number of centroids μ_h are found in X_b based on the k-means clustering algorithm, and the width σ_g is calculated by equation (6);
 - 6: **repeat**()
 - 7: Take a sample x_{ij} in X_b ;
 - 8: $net_{ikj} = \text{relu}(\sum_{l=1, l \neq j}^s w_{lk}^{(1)} \cdot x_{il} + b_k^{(1)}), j=1, 2, \dots, s, k=1, 2, \dots, m_1$;
 - 9: $net_{igj} = \exp\left[-\frac{\|x_{ij} - \mu_g\|}{2\sigma_g^2}\right], j=1, 2, \dots, s, g=1, 2, \dots, m_2$;
 - 10: $y_{ij} = \sum_{k=1}^{m_1} w_{kj}^{(2)} net_{ikj} + b_j^{(2)}, j=1, 2, \dots, s$;
 - 11: $r_{ij} = \sum_{g=1}^{m_2} w_{gj}^{(2)} net_{igj} + b_j^{(2)}, j=1, 2, \dots, s$;
 - 12: Minimization objective function equation and updates the model weights w_k and threshold b_k ;
 - 13: **if** x_{ij} is the sample containing the missing values **then**
 - 14: Update the missing value variables in x_{ij} based on Adam optimization algorithm;
 - 15: **end if**
 - 16: Continue to take the next sample in X_b ;
 - 17: **until** After traversing all samples in X_b
 - 18: **until** Termination of training conditions
-

5 Experiments

In this section, we first conduct experiments on four UCI (University of California Irvine) datasets to evaluate the performance of the proposed method. Besides that, we perform extensive additional experiments on three more complex real datasets to analyze the effectiveness of our model, and the effectiveness of the model was verified by comparing the filling performance with the mean filling method, Autoencoder [5], and CE-AANN [11].

Firstly, various types of deep learning models were constructed based on Tensorflow, including the proposed FFEAM, and the Scikit-learn machine

Table 1 Description of the UCI experimental dataset

| Data set name | Sample size | Number of attributes |
|---------------|-------------|----------------------|
| Iris | 150 | 4 |
| Wine | 178 | 14 |
| Cloud | 1024 | 10 |
| Seeds | 210 | 7 |

Source: The data in the above table are all from the public UCI dataset:
<https://archive.ics.uci.edu/ml/index.php>

Table 2 Description of complex experimental dataset

| Data set name | Sample size | Number of attributes |
|--|-------------|----------------------|
| Traffic data of Baoan District ¹ | 1102 | 10 |
| Beijing PM2.5Data Data Set ² | 43824 | 13 |
| AI4I 2020 Predictive Maintenance Dataset Data Set ³ | 10000 | 14 |

¹The data comes from traffic flow data in Baoan district released by the Shenzhen municipal government's open platform:

https://opendata.sz.gov.cn/data/dataSet/toDataDetails/29200_2803199

²The data comes from Beijing's air quality data set: <http://www.bjmemc.com.cn/>

³This data comes from the AI4I 2020 Predictive Maintenance dataset: <https://archive.ics.uci.edu/ml/datasets/AI4I+2020+Predictive+Maintenance+Dataset#>

learning library was used to construct the mean-fill model, and all experiments were conducted on a PC computer with an operating system of Windows 10 Professional, a processor of Intel(R) Core(TM) i7-7700HQ CPU @2.80 GHz quad-core, 16 GB of RAM (DDR4 2400 MHz), and SD8SN8U- 128G -1006 (128 GB) as the main hard disk.

5.1 Datasets

The first four datasets used in the experiments are open-source datasets originating from UCI, as detailed in Table 1, and the experiments were conducted by randomly removing some existing values from the complete data, thus constructing incomplete datasets with missing rates set to 20%, 30%, 40%, and 50%, respectively.

In addition, extensive experiments were also conducted on three more complex real datasets (missing rate set to 20%), as detailed in Table 2. the first dataset is the traffic flow data of Baoan district released by the Shenzhen government open platform in China, which spans from November 2017 to May 2021, and contains 10 attributes with a total of 1102 samples. The second one is the Beijing PM2.5Data Data Set, which contains air quality data of Beijing from 2010-2014, with a time interval of 1 hour, 13 attributes, and 43824 samples. The third dataset is the AI4I 2020 Predictive Maintenance Dataset, which is a comprehensive dataset reflecting real predictive maintenance data encountered in the industry, and contains 14 attributes with 10,000 samples.

5.2 Baseline model and hyperparameter settings

To validate the filling performance of the model, FFEAM was compared with three benchmark models of mean filling (Means), Autoencoder [5], and CE-AANN [11].

Means: a classical traditional statistical filling method where numerical data is filled with the average of all existing values in the incomplete attribute column.

AE [5]: Filling model based on classical autoencoder, which fills the missing values by reproducing the values of the input at the output.

CE-AANN [11]: a correlation-enhanced self-encoder filling model proposed by Lai et al.

To ensure the fairness of the experiments, the base hyperparameters of the benchmark comparison model and the FFEAM model were the same for each dataset with different missing rates, specifically set as follows: learning rate of 0.1, number of training iterations of 1000, batch size of 20, and the total number of hidden layer neurons of 20. Since in the correlation-enhanced self-encoder model, two types of hidden layer neurons are contained, the specific hidden layer The neuron assignments are both $m_1=10$ and $m_2=10$. Adam function is used as the training optimizer for all models.

5.3 Evaluation Indicators

Root Mean Square Error (RMSE) and Mean Absolute Error (MAE) are used as evaluation indexes for filling performance, and the formulas for RMSE and MAE are Equation (12) and (13), respectively.

$$RMSE = \sqrt{\frac{1}{n} \sum_{i=1}^n (x_i - y_i)^2}, \quad (12)$$

$$MAE = \frac{1}{n} \sum_{i=1}^n \|x_i - y_i\|, \quad (13)$$

In Equation (12) and (13), n is the total number of samples, y_i denotes the filled value, and x_i denotes the true value corresponding to that filled value.

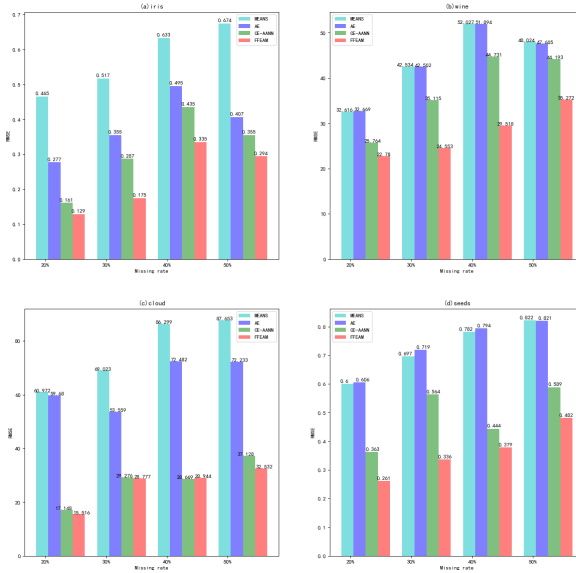
5.4 Analysis of experimental results

Experiments were first conducted based on four UCI datasets, and Table 3 depicts the filling errors of different models for different datasets with different missing rates. From Table 3, it can be seen that FFEAM outperforms the other comparison models in terms of missing value filling. Compared with the classical mean-value filling method and the benchmark AE filling model, FFEAM achieves the lowest RMSE and MAE with higher filling accuracy under different missing rate conditions. Based on the comparison of the experimental results of FFEAM and CE-AANN, it can be seen that the filling accuracy of FFEAM is improved in all four datasets with different missing rates. Taking

Table 3 Comparison of filling errors of different models

| Data set name | Model name | RMSE | | | | MAE | | | |
|---------------|------------|---------------|---------------|---------------|---------------|--------------|--------------|--------------|--------------|
| | | 20% | 30% | 40% | 50% | 20% | 30% | 40% | 50% |
| Iris | MEANS | 0.465 | 0.517 | 0.633 | 0.674 | 0.149 | 0.205 | 0.275 | 0.328 |
| | AE | 0.277 | 0.355 | 0.495 | 0.407 | 0.083 | 0.126 | 0.205 | 0.199 |
| | CE-AANN | 0.161 | 0.287 | 0.435 | 0.355 | 0.049 | 0.089 | 0.145 | 0.144 |
| | FFEAM | 0.129 | 0.175 | 0.335 | 0.294 | 0.041 | 0.064 | 0.126 | 0.129 |
| Wine | MEANS | 32.616 | 42.534 | 52.027 | 48.024 | 3.405 | 5.035 | 6.931 | 7.420 |
| | AE | 32.669 | 42.502 | 51.894 | 47.605 | 3.432 | 5.056 | 7.007 | 7.469 |
| | CE-AANN | 25.764 | 35.115 | 44.731 | 44.193 | 2.605 | 4.084 | 5.669 | 6.547 |
| | FFEAM | 22.780 | 24.553 | 29.518 | 35.272 | 2.383 | 3.226 | 4.044 | 5.456 |
| Cloud | MEANS | 60.972 | 69.023 | 86.299 | 87.653 | 13.607 | 19.073 | 25.100 | 29.261 |
| | AE | 59.680 | 53.559 | 72.482 | 72.233 | 6.804 | 7.858 | 15.558 | 15.345 |
| | CE-AANN | 17.148 | 29.276 | 28.669 | 37.128 | 3.473 | 5.255 | 6.504 | 10.627 |
| | FFEAM | 15.516 | 28.777 | 28.944 | 32.532 | 2.942 | 5.388 | 5.920 | 8.655 |
| Seeds | MEANS | 0.600 | 0.697 | 0.782 | 0.822 | 0.155 | 0.220 | 0.292 | 0.332 |
| | AE | 0.606 | 0.719 | 0.794 | 0.821 | 0.158 | 0.234 | 0.299 | 0.339 |
| | CE-AANN | 0.363 | 0.564 | 0.444 | 0.589 | 0.073 | 0.141 | 0.147 | 0.199 |
| | FFEAM | 0.261 | 0.336 | 0.379 | 0.482 | 0.066 | 0.109 | 0.127 | 0.179 |

the 20% missing rate as an example, the RMSE values of FFEAM are reduced by 0.032, 2.984, and 0.102 compared with CE-AANN on the Iris, Wine, Cloud, and Seeds datasets, respectively. and MAE decreased by 0.008, 0.222, 0.531, and 0.007, respectively.

**Fig. 3** Comparison of RMSE of different models on four UCI datasets

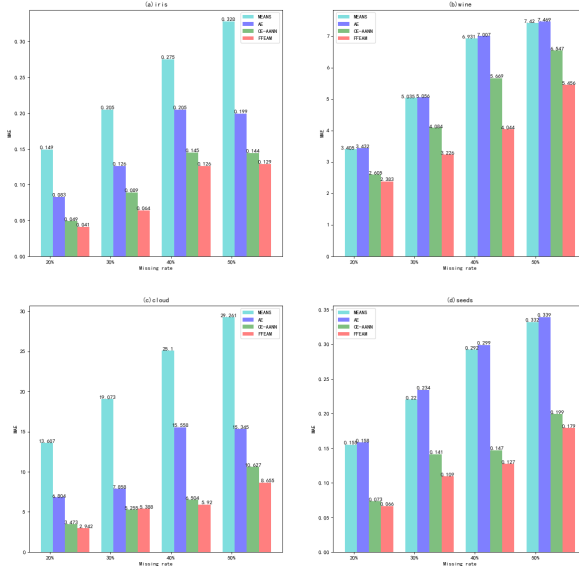


Fig. 4 Comparison of MAE of different models on four UCI datasets

Figure 3 shows the differences in RMSE metrics of the four models on the different datasets, and Figure 4 shows the differences in MAE metrics. According to Figure 3 and Figure 4, it can be seen that the error metrics of AE are close to Means in Wine and Seed datasets, while in the other two datasets, the error of AE decreases compared to Means, indicating that the filling effect of AE is better than Means, and it also shows that AE itself has self-tracking and lacks the ability to discover the correlations and common features among attributes. In addition, most of the suboptimal results are from CE-AANN, which indicates that the filling effect of CE-AANN is generally better than Means and AE although it is not as good as FFEAM, mainly because the model effectively reduces the self-tracking property of the model by introducing de-tracking neurons in the hidden layer, and improves the ability of the model to explore data correlation features. FFEAM achieves the optimal results, mainly because the model has a better fusion learning ability of data correlation features and common features, which further improves the performance of the missing values filling model.

In addition, three more complex real dataset comparison experiments were conducted, based on the traffic flow data of Baoan District, Beijing PM2.5Data Data Set and AI4I 2020 Predictive Maintenance Dataset Data Set, and the incomplete dataset with 20% missing rate was randomly constructed and compared with the three benchmark models. The experimental results obtained are shown in Table 4. From Table 4, it can be seen that the performance of FFEAM in filling the missing values on the real dataset is also better than the benchmark models, with the lowest RMSE and MAE, in which the RMSE of FFEAM is reduced by 1094.681, 1101.336, and 473.904 compared with MEANS, AE,

Table 4 Comparison of filling errors of different models in real data sets

| Data set name | Model Name | RMSE | MAE |
|---|------------|----------------|---------------|
| Traffic data of Baoan District | MEANS | 1687.9270 | 286.815 |
| | AE | 1694.582 | 278.533 |
| | CE-AANN | 1067.15 | 158.45 |
| | FFEAM | 593.246 | 85.458 |
| Beijing PM2.5Data Data Set | MEANS | 13.746 | 1.541 |
| | AE | 13.767 | 1.568 |
| | CE-AANN | 12.793 | 1.484 |
| | FFEAM | 12.107 | 1.321 |
| AI4I 2020 Predictive Maintenance Dataset Data Set | MEANS | 24.716 | 3.183 |
| | AE | 24.714 | 3.195 |
| | CE-AANN | 21.633 | 3.153 |
| | FFEAM | 15.426 | 2.601 |

and CE-AANN, respectively, in the experimental traffic flow data of Baoan district. MAE decreased by 201.357, 193.075, and 72.992 compared to MEANS, AE, and CE-AANN, respectively. In the Beijing PM2.5Data Data Set experiment, the RMSE of FFEAM decreased by 1.639, 1.660, and 0.686 compared to MEANS, AE, and CE-AANN, respectively. In the AI4I 2020 Predictive Maintenance Dataset Data Set, the RMSE of FFEAM was reduced by 9.29, 9.288, and 6.207 compared to MEANS, AE, and CE-AANN, respectively; the MAE was reduced by 0.220, 0.247, and 0.163 compared to MEANS, AE, and CE-AANN, respectively. The validity of the FFEAM model was verified by the reduction in MAE by 0.582, 0.594, and 0.552 compared to MEANS, AE, and CE-AANN, respectively.

Figure 5 shows the differences in RMSE and MAE metrics for the four comparison models on three complex real data sets. The visual comparison analysis in the figure shows that MEANS and AE perform comparable results, and their RMSE and MAE are not very different, while the CE-AANN model improves the effect of the first two models to some extent, and the RMSE and MAE are significantly lower than both MEANS and AE. However, the optimal results on all three real data sets come from the proposed model FFEAM in this paper.

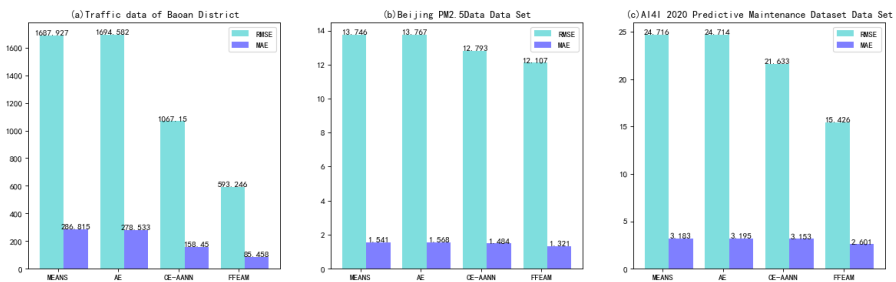
**Fig. 5** Comparison histogram of filling errors of different models in real data sets

Table 5 Comparison of filling errors for different m_1 and m_2 assignments

| m_1, m_2 | RMSE | | | | MAE | | | |
|------------|--------------|--------------|--------------|--------------|--------------|--------------|--------------|--------------|
| | 20% | 30% | 40% | 50% | 20% | 30% | 40% | 50% |
| 5,15 | 0.205 | 0.218 | 0.425 | 0.385 | 0.058 | 0.085 | 0.147 | 0.149 |
| 6,14 | 0.145 | 0.188 | 0.422 | 0.340 | 0.045 | 0.073 | 0.138 | 0.141 |
| 7,13 | 0.139 | 0.183 | 0.379 | 0.348 | 0.043 | 0.071 | 0.123 | 0.145 |
| 8,12 | 0.133 | 0.168 | 0.369 | 0.344 | 0.042 | 0.067 | 0.30 | 0.137 |
| 9,11 | 0.128 | 0.171 | 0.320 | 0.311 | 0.040 | 0.068 | 0.117 | 0.131 |
| 10,10 | 0.129 | 0.175 | 0.335 | 0.294 | 0.041 | 0.064 | 0.126 | 0.129 |
| 11,9 | 0.131 | 0.176 | 0.358 | 0.332 | 0.042 | 0.069 | 0.124 | 0.142 |
| 12,8 | 0.137 | 0.177 | 0.393 | 0.333 | 0.043 | 0.070 | 0.128 | 0.138 |
| 13,7 | 0.139 | 0.175 | 0.387 | 0.357 | 0.046 | 0.068 | 0.139 | 0.155 |
| 14,6 | 0.140 | 0.180 | 0.399 | 0.387 | 0.044 | 0.070 | 0.133 | 0.158 |
| 15,5 | 0.141 | 0.182 | 0.407 | 0.402 | 0.045 | 0.070 | 0.127 | 0.154 |

To investigate the effect of the specific assignment of m_1 and m_2 values on the filling effect of the FFEAM model when the total number of neurons in the hidden layer is constant, experiments were conducted on the Iris dataset with different deletion rates. By setting the total number of neurons constant and fixed to 20, i.e., $m_1+m_2=20$, the experimental error results were obtained by changing the ratio of m_1 and m_2 , as shown in Table 5. It can be seen through Table 5 that the optimal results with different deletion rates are mostly clustered around $m_1=9$ and $m_2=11$, and there is not much fluctuation. And combined with Table 3, it can be seen that the worst performance of the FFEAM model with different missing rates is also better than the second-best result of CE-AANN with the same missing rate in Table 3, for example, in the case of 20% missing rate, the highest RMSE of the FFEAM model is 0.145 and the highest MAE is 0.045, while in CE-AANN, the RMSE is 0.161 and the MAE is 0.049, once again validating the filling performance of the FFEAM model.

Figure 6 shows the line graph of filling error comparison for different m_1 and m_2 assignments. Through Fig.6, it can be visualized that the model filling error, with the total number of hidden layer neurons unchanged, first shows a decreasing trend as m_1 increases and m_2 decreases, and then shows an increasing trend when it decreases to a certain value. The main reason is that when the value of m_1 is too small, the number of de-tracking neurons is too small to effectively explore the association features among data attributes, so as the number of m_1 increases, the ability to explore the association features is improved and the model error is reduced. And when the value of m_2 is too small, the number of radial basis function neurons is too small, and the ability of the model to mine the common features of the data is insufficient, which leads to an increase in the model error. Therefore, the proposed mutual design of the two types of neuron hidden layers needs to set the values of m_1, m_2 reasonably in order to support the cooperative fusion learning of data common features and associative features.

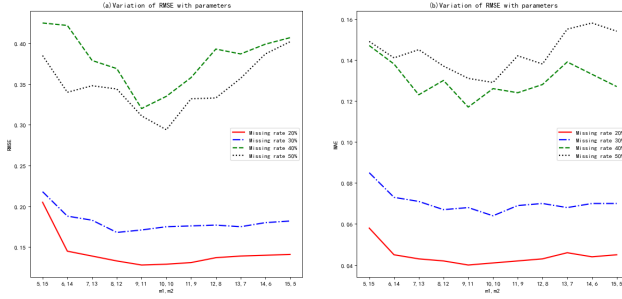


Fig. 6 Comparison of filling errors for different m_1 and m_2 assignments

In summary, combined with the above analysis, the proposed FFEAM has better filling performance than the benchmark models regardless of the settings for different missing rates or the experimental performance on different datasets. The main reason lies in the fact that FFEAM restrains the over-dependence of the network output on the input by introducing de-tracking neurons, i.e., avoiding the invalid constant mapping of directly learning to output reproducing the input, and at the same time, through radial basis function neurons clustering computation is performed on the sample data, and the interaction design between de-tracking neurons and radial basis function neurons allows the model to perform fusion learning of data correlation features and data common features simultaneously.

6 Conclusion

A missing value filling model based on feature fusion enhanced autoencoder is proposed to address the key problems faced by the classical autoencoder model in the application of missing value filling. The model constructed a new hidden layer of neural network by introducing two types of neurons, namely de-tracking neurons and radial basis function neurons, which combine the characteristics of the two types of neurons and exploit the correlation features and common features of input data, so as to achieve multi-dimensional data feature fusion learning and improve the missing filling performance of the model. In addition, MVDC filling strategy was designed, and iterative training is optimized together with the model parameters to improve the model filling effect. The experimental results on seven datasets showed that FFEAM has better filling performance compared to the benchmark models. The current research mostly focuses on numerical missing value filling methods, and how to effectively learn the implicit information inside non-numerical attributes is a key issue to be addressed in future research. Follow up research is to extend the FFEAM model to be able to support filling both numerical and non-numerical missing data to further improve the data quality.

Acknowledgements

This work is supported by the National Key R&D Program of China (No. 2020AAA0105101), the National Natural Science Foundation of China (Nos. 62176221).

References

- [1] Canbek, G.: Gaining insights in datasets in the shade of “garbage in, garbage out” rationale: Feature space distribution fitting. *Wiley Interdisciplinary Reviews: Data Mining and Knowledge Discovery* **12**(3), 1456 (2022)
- [2] Xue, Z., Wang, H.: Effective density-based clustering algorithms for incomplete data. *Big Data Mining and Analytics* **4**(3), 183–194 (2021)
- [3] Vatanen, T., Osmala, M., Raiko, T., Lagus, K., Sysi-Aho, M., Orešič, M., Honkela, T., Lähdesmäki, H.: Self-organization and missing values in som and gtm. *Neurocomputing* **147**, 60–70 (2015)
- [4] García-Laencina, P.J., Sancho-Gómez, J.-L., Figueiras-Vidal, A.R.: Pattern classification with missing data: a review. *Neural Computing and Applications* **19**(2), 263–282 (2010)
- [5] Abdella, M., Marwala, T.: The use of genetic algorithms and neural networks to approximate missing data in database. In: *International Conference on Computational Cybernetic*, pp. 207–212 (2005)
- [6] Liu, K., Lu, N., Wu, F., Zhang, R., Gao, F.: Model fusion and multi-scale feature learning for fault diagnosis of industrial processes. *IEEE Transactions on Cybernetics* (2022)
- [7] Kabir, S., Farrokhvar, L.: Non-linear missing data imputation for healthcare data via index-aware autoencoders. *Health Care Management Science*, 1–14 (2022)
- [8] Lai, X., Wu, X., Zhang, L., Lu, W., Zhong, C.: Imputations of missing values using a tracking-removed autoencoder trained with incomplete data. *Neurocomputing* **366**, 54–65 (2019)
- [9] Ravi, V., Krishna, M.: A new online data imputation method based on general regression auto associative neural network. *Neurocomputing* **138**, 106–113 (2014)
- [10] Gautam, C., Ravi, V.: Counter propagation auto-associative neural network based data imputation. *Information Sciences* **325**, 288–299 (2015)

- [11] Lai, X., Wu, X., Zhang, L., Zhang, G.: Imputation using a correlation-enhanced auto-associative neural network with dynamic processing of missing values. In: International Symposium on Neural Networks, pp. 223–231 (2019)
- [12] LIU, X., DU, S., TENG, F., LI, T.: A missing value filling model based on feature fusion enhanced autoencoder. in: 15th International FLINS Conferences on Machine learning, Multi agent and Cyber physical systems (2022)
- [13] Hamzah, F.B., Hamzah, F.M., Razali, S.M., Samad, H.: A comparison of multiple imputation methods for recovering missing data in hydrological studies. *Civil Engineering Journal* **7**(9), 1608–1619 (2021)
- [14] Alasadi, S.A., Bhaya, W.S.: Review of data preprocessing techniques in data mining. *Journal of Engineering and Applied Sciences* **12**(16), 4102–4107 (2017)
- [15] Rumaling, M.I., Chee, F.P., Dayou, J., Chang, J., Sentian, J.: Missing value imputation for pm10 concentration in sabah using nearest neighbour method (nnm) and expectation-maximization (em) algorithm. *Asian Journal of Atmospheric Environment* **14**(1), 62–72 (2020)
- [16] Ma, B., Li, C., Jiang, L.: A novel ground truth inference algorithm based on instance similarity for crowdsourcing learning. *Applied Intelligence*, 1–13 (2022)
- [17] Tutz, G., Ramzan, S.: Improved methods for the imputation of missing data by nearest neighbor methods. *Computational Statistics & Data Analysis* **90**, 84–99 (2015)
- [18] Wang, M., Li, D., Qi, K., Xue, C., Yang, E.: Sknn algorithm for filling missing oil data based on knn. *IOP Conference Series Materials Science and Engineering* **612**, 032099 (2019)
- [19] Gajawada, S., Toshniwal, D.: Missing value imputation method based on clustering and nearest neighbours. *International Journal of Future Computer and Communication* **1**(2), 206–208 (2012)
- [20] Li, D., Zhang, H., Li, T., Bouras, A., Yu, X., Wang, T.: Hybrid missing value imputation algorithms using fuzzy c-means and vaguely quantified rough set. *IEEE Transactions on Fuzzy Systems* **PP**, 1–1 (2021)
- [21] Tang, S., Yuan, S., Zhu, Y.: Deep learning-based intelligent fault diagnosis methods toward rotating machinery. *Ieee Access* **8**, 9335–9346 (2019)
- [22] Al-Kaabi, K., Monsefi, R., Zabihzadeh, D.: A framework to enhance

generalization of deep metric learning methods using general discriminative feature learning and class adversarial neural networks. *Applied Intelligence*, 1–19 (2022)

- [23] Saad, M., Chaudhary, M., Karray, F., Gaudet, V.: Machine learning based approaches for imputation in time series data and their impact on forecasting. In: *IEEE International Conference on Systems, Man, and Cybernetics (SMC)*, pp. 2621–2627 (2020)
- [24] Zhao, R., Yan, R., Chen, Z., Mao, K., Wang, P., Gao, R.X.: Deep learning and its applications to machine health monitoring. *Mechanical Systems and Signal Processing* **115**, 213–237 (2019)